16th World Conference on Earthquake, 16WCEE 2017

Santiago Chile, January 9th to 13th 2017

Paper N° 2514

Registration Code: S-Z1450120510

NEW OPENSEES MODELS FOR SIMULATION OF NONLINER FLEXURAL AND SHEAR-FLEXURAL BEHAVIOR OF RC WALLS AND COLUMNS

K. Kolozvari(1), K. Orakcal(2), J. W. Wallace(3)

(1) *Assistant Professor, California State University, Fullerton, CA, USA, kkolozvari@fullerton.edu*
(2) *Associate Professor, Bogazici University, Istanbul, Turkey, kutay.orakcal@boun.edu.tr*
(3) *Professor, University of California, Los Angeles, CA, USA, wallacej@ucla.edu*

Abstract

Existing approaches used to model the lateral load versus deformation responses of reinforced concrete (RC) members typically assume uncoupled axial/flexural and shear responses. A novel analytical model that captures interaction between axial/flexural and shear behavior in RC walls and columns under reversed-cyclic loading conditions has been developed and implemented into the computational platform OpenSees. The proposed modeling approach incorporates RC panel behavior described with a constitutive fixed-strut-angle panel model into a two-dimensional Multiple-Vertical-Line-Element-Model (MVLEM) formulation. This paper describes new classes added to the existing OpenSees library including: 1) baseline MVLEM element with uncoupled axial/flexural and shear behavior, 2) Shear-Flexure-Interaction MVLEM (SFI-MVLEM) element, 3) 2-D RC panel model based on the fixed-strut-angle approach, 4) uniaxial material model for concrete, and 5) uniaxial material model for steel. In addition, validation of the analytical models for quasi-static analysis of: i) RC column specimen using the SFI-MVLEM, ii) a relatively slender RC wall specimen with flexure-dominated response using the MVLEM, and iii) a moderate-aspect-ratio RC wall specimen with flexure-shear dominated response using the SFI-MVLEM, are presented. Response comparisons reveal that the implemented analytical models capture well the experimentally-measured behavior of RC structural walls and columns. Based on the comparisons presented, model capabilities are assessed and potential model improvements are identified.

Keywords: Reinforced concrete elements; Analytical modeling; Shear-flexure interaction; OpenSees; Earthquake eng.;

1. Introduction

Reinforced concrete (RC) structural walls and columns are often used as the primary structural elements for resisting earthquake actions in buildings (e.g., core wall or wall-frame dual systems) and bridges (e.g., bridge columns). Behavior of RC walls and columns is generally classified according to their aspect ratio (h/l), or shear-span-to-depth ratio (M/Vl), as either shear-controlled (aspect ratios less than approximately 1.0 to 1.5) or flexure-controlled (aspect ratios greater than 2.5 to 3.0). For walls and columns between these aspect ratios, although flexural yielding is expected, nonlinear shear deformations may be significant and lead to reduced lateral stiffness, strength and ductility.

Experimental results on RC walls have shown that flexural and shear yielding occur near-simultaneously even when the wall nominal shear strength is as much as twice the shear developed at flexural yielding [1], suggesting that there is an interaction between nonlinear flexural and shear modes of behavior, commonly referred to as shear-flexure interaction (SFI), which has been observed in a number of experimental studies on RC walls [2, 3, 4]. Experimental data showed that the contribution of shear deformations to lateral displacements of a wall generally increases with decrease of wall aspect ratio (e.g., from 10% for h/l = 3.0 [2] to 50% for h/l = 1.5 [4]). Similarly, experiments on RC columns have shown that the shear and flexural capacities of RC columns could be reduced due to SFI comparing to pure bending case, and that the shear displacements can be significant even when the failure is not governed by shear behavior [5, 6].

Modeling approaches currently available for representing the SFI behavior in RC walls [7, 8, 9, 10, 11] and columns [12, 13] are either: 1) empirical (or semi-empirical) or have cumbersome formulations, 2) capable of simulating monotonic responses only, 3) not been sufficiently validated due to lack of detailed experimental data characterized with SFI, and 4) not been implemented in computational platforms available to public use. Given these shortcomings of current analytical models, a research project was initiated to develop and implement into the computational platform OpenSees [14] an analytical modeling approach that incorporates the interaction between axial/flexure and shear behavior in RC members subjected to cyclic loading, as well as to calibrate and validate the model using experimental data obtained from tests on RC structural walls and columns. The proposed modeling approach was originally developed in Matlab (Math-Works, Inc.) and validated against detailed experimental data obtained for five medium-rise RC wall specimens [4] that experienced significant SFI [15, 16]. This paper focuses primarily on description of the analytical models for RC structural components implemented into OpenSees and examples of model applications to analysis of RC walls and columns.

The following new classes are added to the existing OpenSees library (names of analytical models have embedded links to OpenSeesWiki user manuals):

1. *Element* MVLEM: macroscopic element with uncoupled flexural and shear behavior
2. *Element* SFI_MVLEM*:* macroscopic element with shear-flexure interaction
3. *nDMaterial* FSAM: plane-stress RC panel constitutive behavior
4. *uniaxialMaterial* ConcreteCM: uniaxial material model for concrete
5. *uniaxialMaterial* SteelMPF: uniaxial material model for steel

Brief description of the models is presented here, whereas details about OpenSees implementation and application can be found in PEER report by Kolozvari et al [17].

2. Description of the Analytical Models

2.1 Flexural Element (MVLEM)

The *MVLEM* element implemented in OpenSees represents a two-dimensional Multiple-Vertical-Line-Element-Model [18] [19] for simulation of flexure-dominated behavior of RC members. A single model element incorporates six global degrees of freedom (DOFs) as illustrated in Fig. 1a. The axial/flexural response of the *MVLEM* is simulated by a series of uniaxial elements (or macro-fibers) connected to the rigid beams at the top and bottom (e.g., floor) levels, whereas the shear response is described by a shear spring located at height *ch* from the bottom of the model element. Shear and flexural responses of the model element are uncoupled. The relative rotation between top and bottom faces of the wall element occurs around the point located on the central axis of the element at height *ch* (Fig. 1a); a value of $c = 0.4$ was recommended by Vulcano et al. [18] based on comparison of the model response with experimental results.

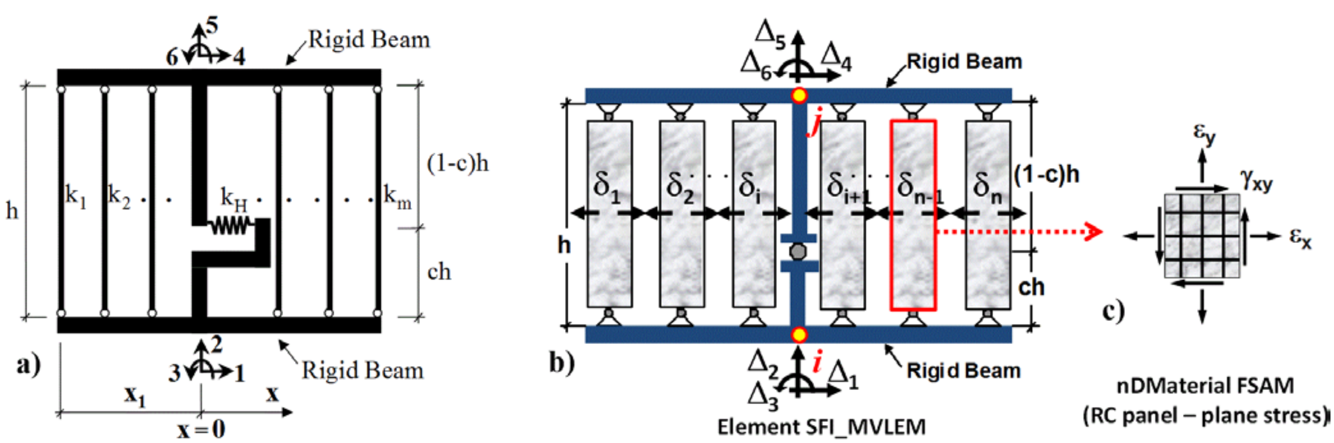

Fig. 1 –Modeling approaches: a) MVLEM element, b) SFI_MVLEM element, c) RC panel model

2.2 Shear-Flexure Interaction Element (SFI_MVLEM)

Shear-Flexure Interaction Multiple-Vertical-Line-Element Model (SFI-MVLEM, [15, 16]) captures interaction between axial/flexural and shear behavior of RC structural walls and columns under cyclic loading. The

SFI_MVLEM element implemented in OpenSees (Fig. 1b) incorporates 2-D RC panel behavior described by the Fixed-Strut-Angle-Model (*FSAM*, Fig. 1c [20, 21]), into a 2D macroscopic fiber-based model (*MVLEM*). The interaction between axial and shear behavior is captured at each RC panel (macro-fiber) level, which further allows interaction between shear and flexural behavior at the *SFI_MVLEM* element level.

Based on deformations at six degrees of freedom located at the top and bottom of the model element (Fig. 1b), axial strains ε_y of each RC panel are calculated using the plane sections assumption, shear strains γ_{xy} of each RC panel are derived assuming their uniform distribution across the wall cross-section, whereas axial strains ε_x of each RC panel element are obtained assuming that the sum of horizontal stresses associated with steel and concrete (i.e., resultant stress σ_x) are equal to zero. Similarly to baseline MVLEM formulation, relative rotations and shear deformations between the element top and bottom faces occur around a point on the element central axis at height *ch*. Shear spring is removed in the SFI-MVLEM since shear stiffness and strength of the element evolve according to computed RC panel responses and assumed material behavior, as opposed to use of a backbone relation in typical fiber-based formulation (e.g., MVLEM, displacement-based beam-column element).

2.3 Constitutive Reinforced Concrete Panel Model (FSAM)

Constitutive RC panel model FSAM (Fig. 2) is a plane-stress constitutive model for simulating the behavior of RC panel elements under generalized, in-plane, reversed-cyclic loading conditions [20, 21]; FSAM model formulation is incorporated in OpenSees as a *nDMaterial FSAM*. In the FSAM, the strain fields acting on concrete and reinforcing steel components of an RC panel are assumed to be equal to each other, implying perfect bond assumption between concrete and reinforcing steel bars. While the reinforcing steel bars develop uniaxial stresses under strains in their longitudinal direction, the behavior of concrete is defined using stress–strain relationships in biaxial directions, the orientation of which is governed by the state of cracking in concrete. Although the concrete stress–strain relationship is fundamentally uniaxial in nature, it also incorporates biaxial softening effects including compression softening and biaxial damage. Material models used in the FSAM formulation are constitutive model for concrete by Chang and Mander [22] and stress-strain relationship for steel proposed by Menegotto and Pinto [23]. For transfer of shear stresses across the cracks, a friction-based elasto-plastic shear aggregate interlock model is adopted [21], together with a linear elastic model for representing dowel action on the reinforcing steel bars [24].

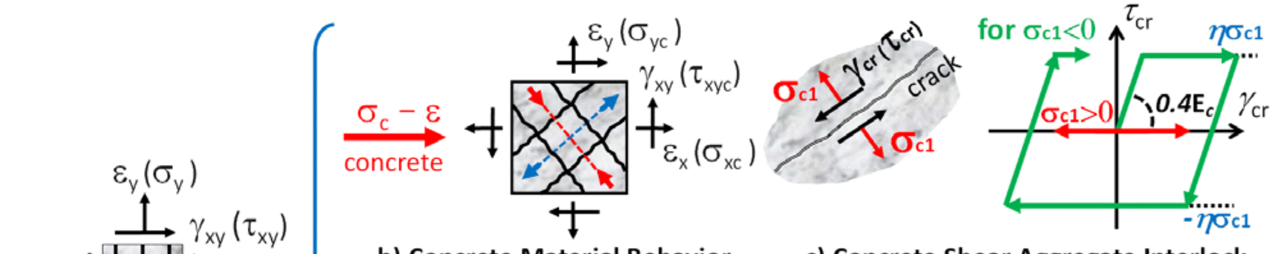

[redacted]

Fig. 2 – Behavior and modeling parameters of the FSAM constitutive RC panel model

2.4 Uniaxial Concrete Constitutive Model (ConcreteCM)

Uniaxial hysteretic constitutive model for concrete developed by Chang and Mander [22] is a refined, rule-based, generalized, and non-dimensional constitutive model that allows calibration of the monotonic and hysteretic material modeling parameters, and can simulate the hysteretic behavior of confined and unconfined, ordinary and high-strength concrete, in both cyclic compression and tension. The model addresses important behavioral features, such as continuous hysteretic behavior under cyclic compression and tension, progressive stiffness degradation associated with smooth unloading and reloading curves at increasing strain values, and gradual crack closure effects. Details of the model can be found in Chang and Mander [22].

Constitutive material model by Chang and Mander is implemented in OpenSees as *uniaxialMaterial ConcreteCM* and incorporates the unloading/reloading rules defined originally by Chang and Mander [22], as opposed to *Concrete07*, which adopts simplified hysteretic rules (Fig. 3a). Besides common input parameters used to define compression and tension envelopes of the constitutive relationship, an optional input parameter is introduced in the *ConcreteCM* model implemented in OpenSees to allow control over the plastic stiffness upon unloading from tension envelope (E_{pl}^{+}), which influences the intensity of gap closure (more gradual versus less gradual) in the stress-strain behavior of concrete (Fig. 3b), which in-turn could influence the level of pinching in the lateral load-displacement behavior of a RC member, as illustrated for a slender wall in Section 3.2.1.

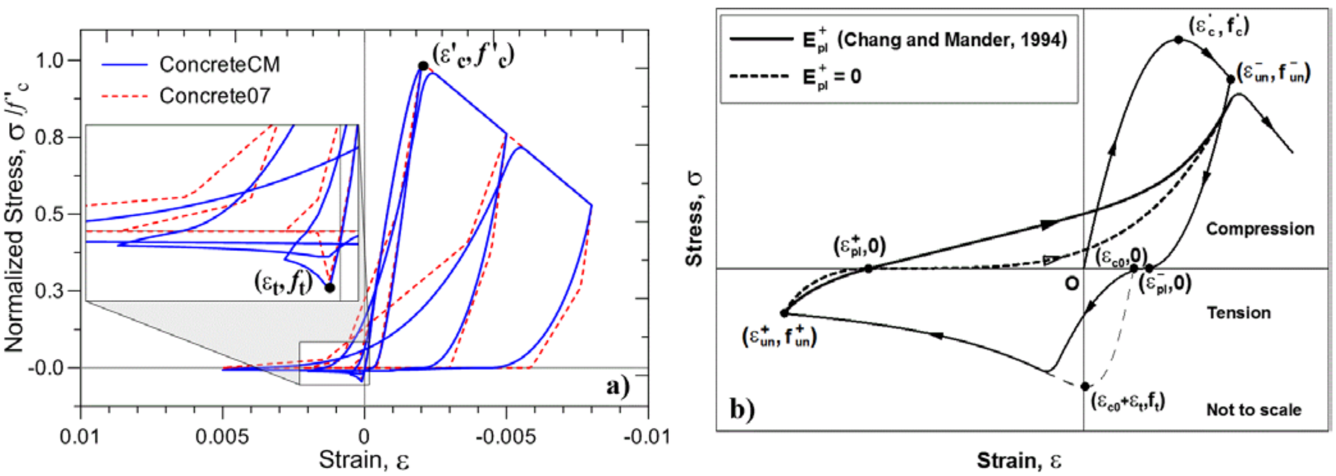

Fig. 3 – Hysteretic constitutive model for concrete by Chang and Mander (1994): a) Sample stress-strain relationship (*ConcreteCM* versus *Concrete07*), b) Effect of plastic stiffness upon unloading from tension envelope (E_{pl}^{+}) on crack closure

2.5 Uniaxial Steel Constitutive Model (SteelMPF)

Uniaxial constitutive nonlinear hysteretic material model for steel proposed by Menegotto and Pinto [23], and extended by Filippou et al. [25] to include isotropic strain hardening effects, is implemented in this study in OpenSees as *uniaxialMaterial SteelMPF* to simulate the behavior of reinforcement. The model allows calibration of isotropic hardening parameters in both compression and tension. Although this material model is already available in OpenSees (e.g., *Steel02*), the formulation of *SteelMPF* brings several distinctive features compared to the existing models. For example, the implemented model allows definition of different yield stresses and strain hardening ratios for compression and tension, which allows consideration of tension stiffening effects on the tensile stress-strain behavior of reinforcing bars embedded in concrete. As well, the implemented model considers degradation of the cyclic curvature parameter *R* for strain reversals in both pre- and post-yielding regions of the hysteretic stress-strain behavior, which may provide more accurate predictions of the yield capacity of RC structural members under cyclic loading, whereas *Steel02* considers the cyclic curvature degradation after formation of post-yield strains only. Fig. 4a compares strain-stress relationships obtained using *SteelMPF* and *Steel02* for a strain history that includes strain reversals at strain values equal to one-half of the yield strain (e.i., $\varepsilon_r = \pm 0.001 = \varepsilon_y/2$). Furthermore, it has been observed from the strain-stress relationships obtained from quasi-static or dynamic analyses using existing steel models in OpenSees (e.g., *Steel02*) that after partial unloading occurs in a model element caused by dynamic loading or stress re-distribution under quasi-static loading due to concrete cracking or crushing, the Menegotto-Pinto formulation produces stress overshooting in the cyclic stress-strain behavior of reinforcing steel. This overshooting effect is not behavioral and causes non-physical hardening in the stress-strain behavior, upon reloading from the partial unloading loop. This phenomenon is illustrated in Fig. 4b for the *Steel02* model. This anomaly results in overestimation of steel stresses predicted by the *Steel02* model upon return from partial unloading, yielding strain-stress curve that may not represent the physical constitutive behavior of reinforcing steel under cyclic loading. The overshooting effect observed in *Steel02* has been remedied in *SteelMPF* via manipulating the model formulation so that reloading behavior after partial unloading cannot overshoot the previous loading loop in the cyclic stress-strain behavior. The comparison between strain-stress relationships obtained using *SteelMPF* and *Steel02* for a strain history that includes low-amplitude unloading followed by reloading is presented in Fig. 4b.

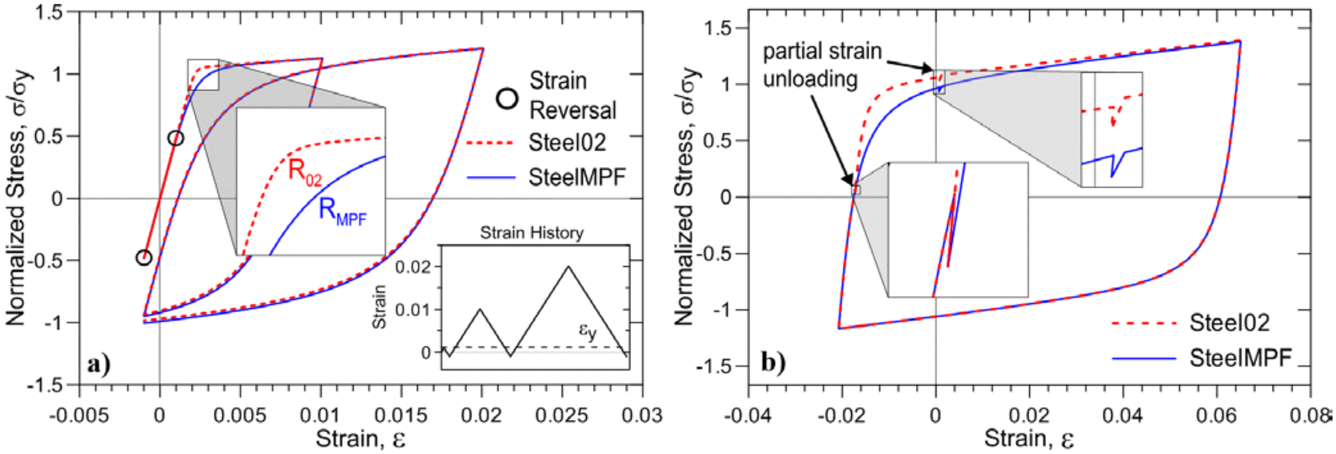

Fig. 4 – Steel02 and SteelMPF: a) Degradation of cyclic curvature in pre-yielding region, b) Stress overshooting upon reloading from low-amplitude unloading

3. Experimental Validation of OpenSees Models

Validation of analytical models described in previous section against experimental results obtained from tests on RC columns and walls are presented in the following section, whereas more detailed information on model descriptions and experimental validation can be found in PEER Report by Kolozvari et al. [17].

3.1 Cyclic Analysis of Reinforced Concrete Column

The SFI-MVLEM model implemented in OpenSees was used to simulate the behavior of a RC column specimen 2CLH18 with rectangular cross-section tested by Lynn et al. [26]. Specimen was tested under double curvature and constant axial load of 503 kN (113 kips, 0.073 $A_g f'_c$) and reversed-cyclic lateral displacement history applied at the top. Specimen cross-section dimensions were 0.46 m × 0.46 (18 in. × 18 in.) with height of 2.95 m (116 in.), resulting in span-to-depth ratio of 3.2. Specimen vertical reinforcement consisted of 8 #8 bars (d_b = 25.4 mm = 1 in.), while horizontal reinforcement were #3 (d_b = 9.5 mm = 0.375 in.) bars spaced at 457 mm (18 in.), corresponding to vertical and horizontal reinforcing ratios equal to 0.0194 and 0.0007, respectively. Concrete compressive strength was 33.1 MPa (4.80 ksi) and steel yielding stress was 331 MPa (48.0 ksi). The specimen experienced shear-flexural failure.

Analytical model of the column specimen was generated in OpenSees using the *SFI-MVLEM* model elements. The specimen was discretized with seven model elements along the height of the column (n = 7) such that height-to-width ratio of each model element is approximately 1.0, and seven RC macro-fibers along the column cross-section (m = 7) based on the number and locations of vertical reinforcing bars, as illustrated in Fig. 5a. The reinforcing ratio in vertical direction for each macro-fiber (RC panel) was obtained based on the areas of vertical reinforcing bars and concrete within the macro-fiber, whereas reinforcing ratio in horizontal direction was obtained based on the area of transverse reinforcement provided within the model element in the direction of loading (e.g., E-W, Fig. 5a). Uniaxial material models for concrete and reinforcing steel were calibrated to match as-tested material properties. Finally, axial load and lateral displacement history matching test conditions were applied at the top node of the analytical models. Additional information about validation of the SFI-MVLEM against experimental results on RC columns with a range of characteristics (cross-section, axial load, aspect ratio) can be found in corresponding PEER Report [17].

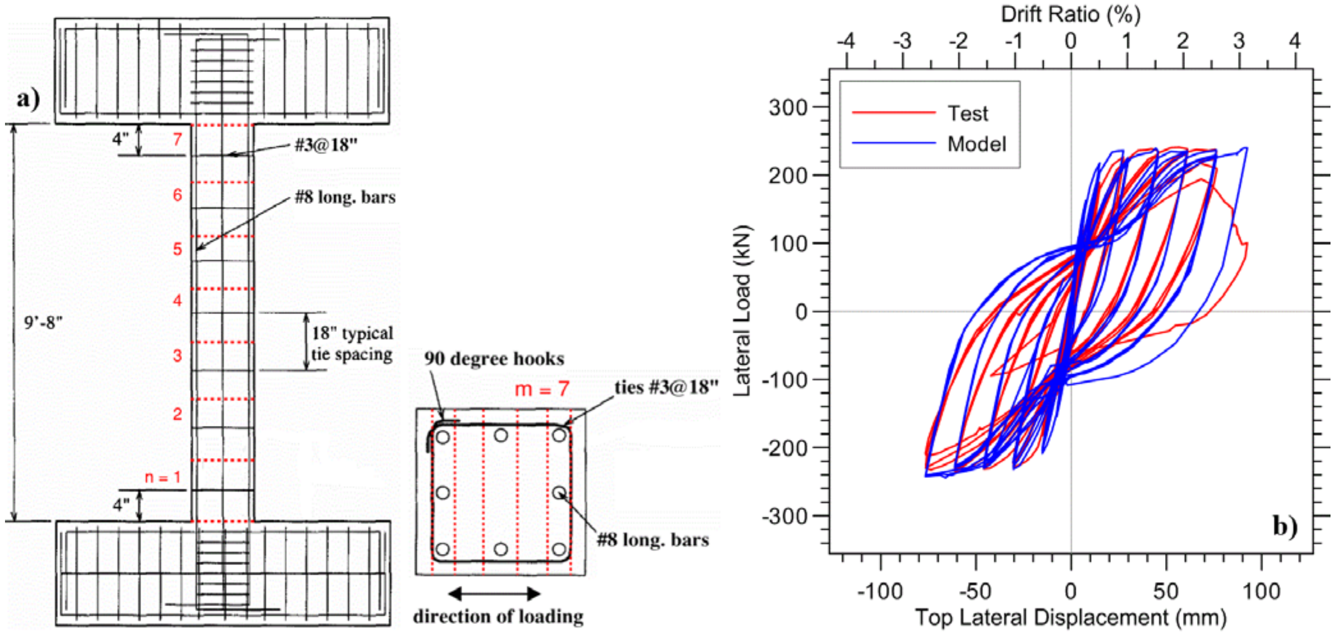

Fig. 5 – Specimen 2CLH18 (Lynn et al. 1996): Specimen geometry and reinforcement, b) Measured and predicted lateral load versus top displacement response

Fig. 5b compares the experimentally-measured and analytically-predicted lateral load versus deformation response for the test specimen considered. As shown in the figure, the analytical model predicts reasonably well the lateral strength under reversed-cyclic loading, and the pinching characteristics of the load-deformation response. Initial stiffness of column specimen is slightly overestimated. Loading and unloading stiffness is reasonably well-predicted by the analytical model. Although the experimentally measured load-deformation behavior of the specimens is generally predicted reasonably well by the *SFI-MVLEM*, including their lateral load capacity, cyclic stiffness degradation and pinching characteristics of the response; strength loss observed in the experiments due to shear-flexure failure was not captured in the analytical results. This model's shortcoming is mainly associated with the inability of the proposed modeling approach to represent strength degradation mechanisms due to simplified shear resisting mechanisms across the cracks implemented in the model formulation, which typically leads to overestimation of the column drift capacity. Future studies will focus on model improvements to address these issues.

3.2 Cyclic Analysis of Reinforced Concrete Walls

3.2.1 Simulation of Flexural Behavior using MVLEM Element

Application of the MVLEM element to simulation of the flexural response of RC walls is illustrated using the wall specimen RW2 tested by Thomsen and Wallace [2]. Specimen RW2 was 2.90 m (144 in.) tall, 1.22 m (48 in.) wide, and 0.10 m (4 in.) thick, resulting in aspect ratio of 3.0. The specimen was subjected to constant axial load of approximately 7% of wall axial load capacity ($0.07\,A_g\,f'_c$) and cyclic lateral displacement history applied at the top of the wall. Mean concrete compressive strengths at the time of testing was approximately 42.8 MPa (6.21 ksi). Longitudinal reinforcement at wall boundaries consisted of 8 - #3 bars (Grade 60, f_y = 414 MPa = 60 ksi), whereas uniformly distributed web reinforcement consisted of two curtains of deformed #2 bars (f_y = 448 MPa = 65 ksi), as shown in Fig. 6. In addition, Fig. 6 displays model discretization of the RW2 cross section, with eight uniaxial elements defined along the length of the wall. The analytical model was discretized along wall height with 16 *MVLEM* elements with element heights in agreement with instrumentation provided on the specimen to allow consistent strain comparisons between model and experimental results. The material models for concrete (*ConcreteCM*) and steel (*SteelMPF*) were calibrated to match as-tested material properties. Only flexural behavior of the wall was predicted using the *MVLEM*. Therefore, large shear stiffness was assigned to the model elements and the experimentally-filtered flexural displacement history was applied at the top of the wall model to compare experimentally measured and analytically predicted flexural responses. Details on specimen RW2 and the test procedure are provided by Thomsen and Wallace [2], whereas detailed information regarding model calibration and experimental validation are presented by Orakcal [28] and Orakcal and Wallace [27].

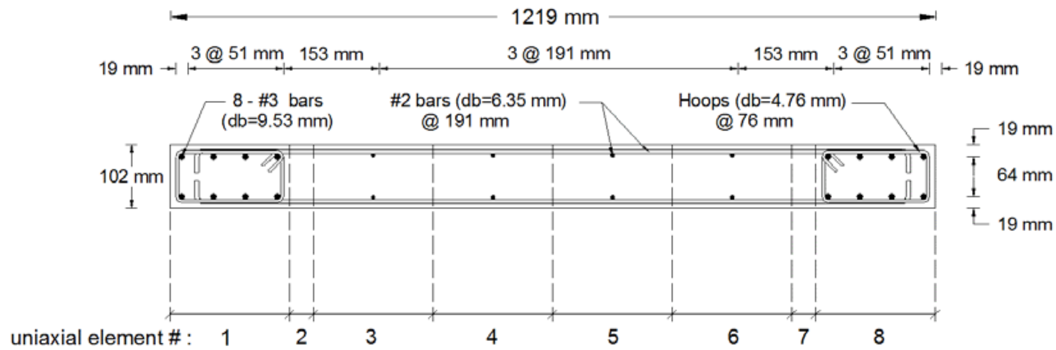

Fig. 6 – Geometry and discretization of Wall Specimen RW2

Fig. 7a compares the flexural load-deformation responses predicted by the *MVLEM* and measured during the test. As shown in the figure, the analytical model captures reasonably well the experimentally measured wall flexural load-deformation behavior. Cyclic properties of the response, including stiffness degradation, hysteretic shape, plastic (residual) displacements, and pinching behavior are accurately represented in the analytical results; therefore, cyclic characteristics of the implemented stress–strain relationships for steel and concrete are suitable for obtaining accurate global response predictions. The lateral capacity of the wall is predicted very closely for most lateral drift levels. The underestimation of the wall capacity at intermediate drift levels in the negative loading direction (e.g., 0.5 to 1.5% drift) can be attributed to the inability of the yield asymptote in stress–strain model for steel in tension to represent the curved strain-hardening region observed in the stress–strain tests for the #3 longitudinal reinforcing bars, as well as uncertainties in calibration of the cyclic parameters govrning the implemented steel stress–strain model (R_0, a_1, and a_2 of *SteelMPF*) and the parameters associated with concrete tensile strength (f_t and ε_t of *ConcreteCM*).

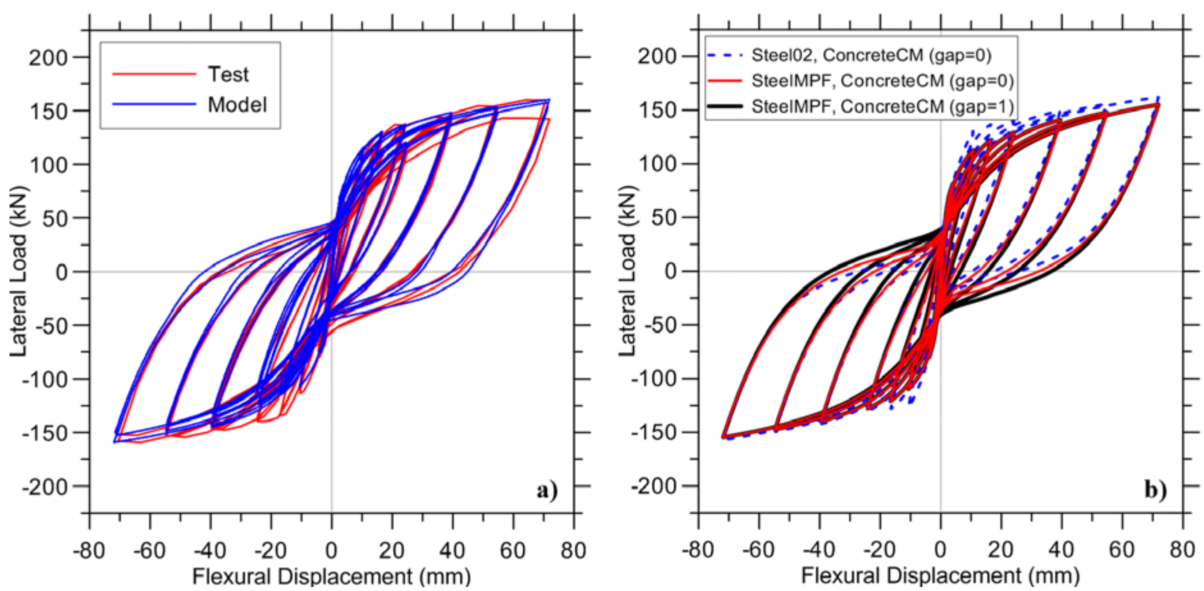

Fig. 7 – Flexural load-deformation behavior for specimen RW2: a) Experimental and analytical responses, b) Response sensitivity to material modeling parameters of concrete and steel

Fig. 7b illustrates the sensitivity of analytical predictions obtained using the *MVLEM* to the optional gap closure parameter of the *ConcreteCM* model mentioned earlier, which allows consideration of different intensities of gradual gap closure in concrete (Fig. 3b), as well as selection of the steel material model *SteelMPF* versus *Steel02*. Note in Fig. 7b that pinching characteristics of the response are slightly more pronounced when less gradual gap closure versus more gradual gap closure (i.e., *gap*=0 versus *gap*=1) is adopted. Fig. 7b also illustrates that the wall yield capacity, as well as pinching characteristics of the behavior predicted by the *MVLEM* vary slightly when *SteelMPF* versus *Steel02* is used; i.e., model with *Steel02* predicts larger yield capacity and more pinching due to different interpretation of parameter controlling cyclic degradation of curvature in the material model formulation as illustrated in Fig. 4a.

3.2.2 Simulation of Shear-Flexural Behavior of a Medium-Rise RC Wall using SFI-MVLEM Element

As an example of applying the *SFI-MVLEM* to predict the pronounced shear-flexure interaction behavior in medium-rise RC walls, behavior of the RC wall specimen RW-A15-P10-S78 [4] tested under constant axial load and cyclic lateral displacement history applied at the top of the wall was predicted using the *SFI-MVLEM* model. The specimen was 0.15 m (6 in.) thick, 1.22 m (48 in.) long, and 1.83 m (72 in.) tall, which corresponds to an aspect (or shear-span-to-depth) ratio of 1.5 (medium-rise wall). Wall boundary reinforcement consisted of four #5 and four #6 bars with typical A706 Grade 60 material properties, whereas web reinforcement consisted of Grade 60 #3 bars placed at 0.13 m (5 in.) spacing in both vertical and horizontal direction (Fig. 8b). Concrete peak compressive strength at the time of testing was equal to 55.78 MPa (8.09 ksi) based on a standard cylinder test. The specimen was subjected to constant axial load of approximately 10% of wall axial capacity.

Parameters of the concrete (*ConcreteCM*) and steel (*SteelMPF*) material models were calibrated to match as-tested material properties. Specimen geometry along the height was discretized using five *SFI-MVLEM* elements as shown in Fig. 8a, where the bottom two elements, 0.30 m (12 in.) high, represented the plastic-hinge region of the wall observed in the experiment. Discretization of the model cross section was performed using five RC panel (macro-fiber) elements, where outer two fibers represented confined wall boundaries and the three inner fibers represented the unconfined web of the wall (Fig. 8b). Detailed information about the test specimen can be found in Tran and Wallace [4], whereas details on model calibration and validation are provided by Kolozvari [24] and Kolozvari et al. [16].

Fig. 8 – Model discretization: a) plan view, b) cross-section

Analytically predicted and experimentally obtained lateral load versus top total displacement responses and wall cracking patterns are compared in Fig. 9, whereas lateral load versus flexural and shear deformations are shown in Fig. 10. As shown in Fig. 9a, the analytical model captures reasonably well the overall load-deformation behavior of Specimen RW-A15-P10-S78, including loading and unloading stiffness, pinching characteristics, and lateral load capacity of the wall in positive loading direction; whereas wall capacity is slightly underestimated in negative loading direction at intermediate drift levels (between 0.5 and 1.5% drift), possibly due to same reasons described in the previous section for Specimen RW2. Significant strength degradation observed during the experiment caused by buckling of vertical reinforcing bars in the wall boundary and shear sliding adjacent to wall base was not captured in analytical results due to inability of the model to simulate these strength loss mechanisms. Fig. 9b reveals that analytically-predicted distribution and orientation of cracks agree well with the experimentally-recorded cracking pattern, indicating that the assumptions related to cracking criteria and crack orientations in the formulation of the FSAM are reasonable.

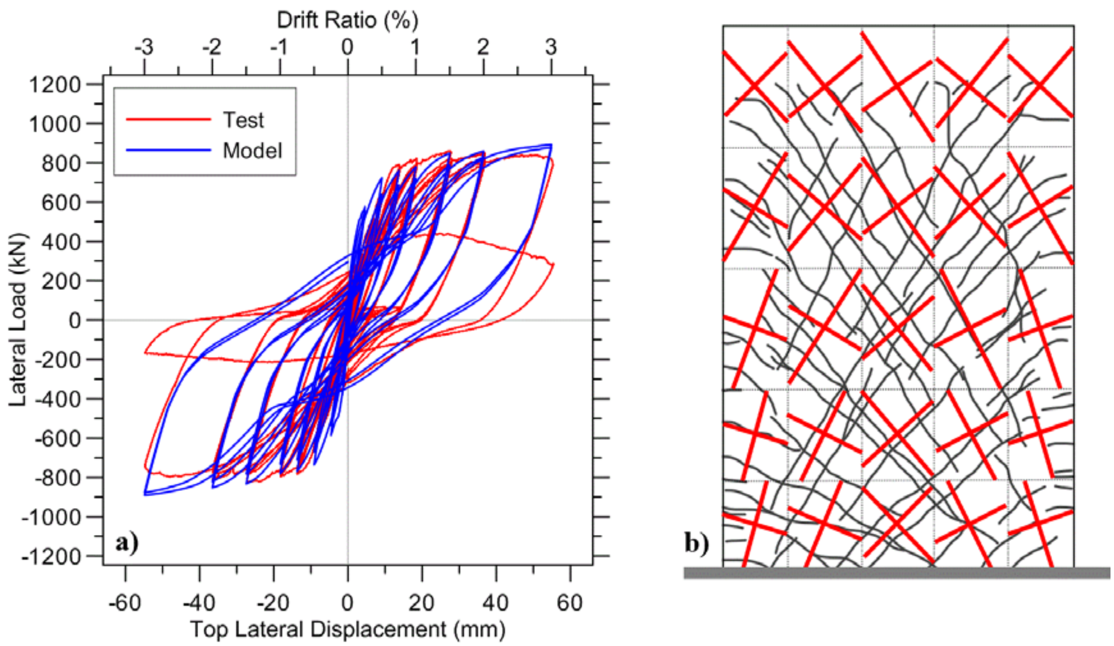

Fig. 9 – Measure and predicted wall responses: a) lateral load versus top displacement, and b) cracking patterns

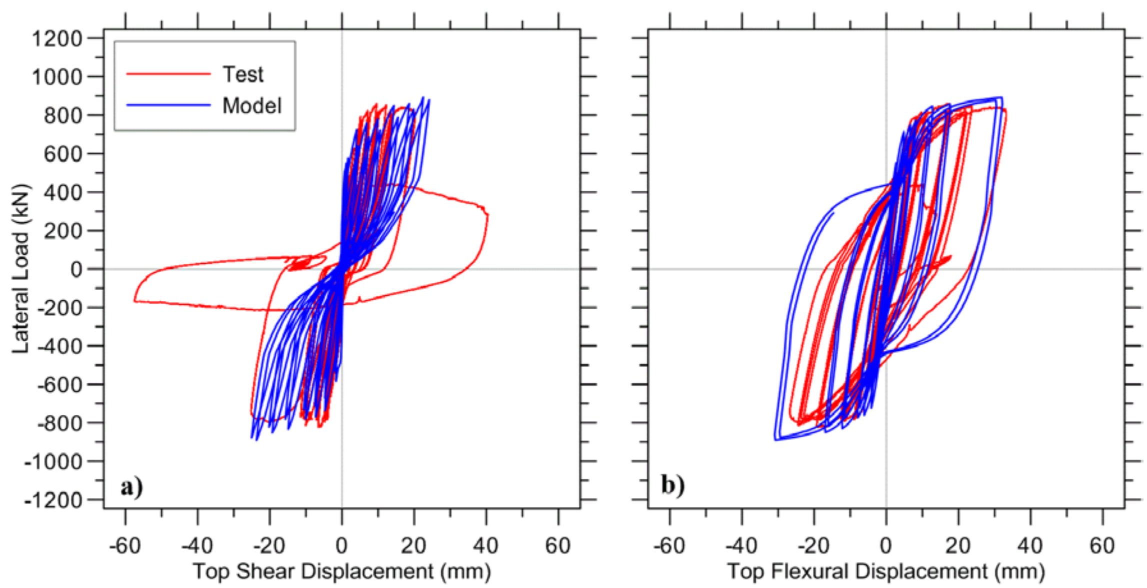

Fig. 10 – Measure and predicted load versus deformation behavior for: a) flexure, and b) shear

As shown in Fig. 10, the analytical model successfully captures the nonlinear flexural and shear deformations and their coupling throughout the entire cyclic loading history. As revealed in both experimental and analytical results, flexural and shear yielding occur almost simultaneously for the wall specimen at a lateral load level of approximately 800 kN (180 kips). In addition, the model successfully reproduces the shapes of the load versus flexural and shear deformation responses, with the flexural response characterized by minimal pinching and shear behavior characterized by a highly-pinched load-deformation response. Although the analytical model captures the flexural stiffness of the wall at all drift levels, shear stiffness is overestimated at drift levels lower than 0.5%. The magnitudes of nonlinear flexural and shear deformation components predicted by the model generally match the experimentally measured values throughout the cyclic loading history. However, as depicted in Fig. 10b, the analytical model underestimates the shear deformations measured during the experiment during the second loading cycle to 3.0% drift in the positive direction because of its inability to capture the shear sliding adjacent to wall base observed during the test, which caused progressively increasing lateral strength degradation. Further information regarding model calibration and validation for this wall specimen, as well as other medium-rise wall specimens, is provided by Kolozvari [24] and Kolozvari et al. [16].

4. Summary and Conclusions

An analytical model that integrates axial/flexural and shear responses and simulates their interaction under cyclic loading conditions has been developed and implemented into the open-source computational platform developed by the Pacific Earthquake Engineering Research (PEER) Center, OpenSees. The proposed analytical model, called the *SFI-MVLEM*, incorporates RC panel behavior described by a fixed-crack-angle modeling approach (FSAM), into the fiber-based Multiple-Vertical-Line-Element-Model (*MVLEM*). The interaction of axial and shear modes of behavior is simulated at the RC panel (macro-fiber) level, which further allows capturing interaction between shear and flexural responses at the model element level. The implementation of the novel shear-flexure interaction model included incorporation of five new features into OpenSess software including: (1) model element based on original formulation of the Multiple-Vertical-Line-Element-Model (*MVLEM*) with uncoupled axial/flexural and shear behavior, (2) model element based on the formulation of Shear-Flexure-Interaction Multiple-Vertical-Line-Element-Model (*SFI-MVLEM*), that captures interaction between nonlinear axial/flexural and shear responses, (3) 2D in-plane constitutive panel model based on a fixed-strut-angle modeling approach (*FSAM*), (4) uniaxial material model for concrete (*ConcreteCM*), and (5) uniaxial material model for steel (*SteelMPF*). Examples of applications of new analytical models to simulation of nonlinear behavior of RC walls and columns are provided. Detailed user manuals for new OpenSees classes are available on the OpenSees Wiki web page.

The analytical models implemented into OpenSees were validated against experimental results obtained from tests on RC column rectangular cross section, as well as slender RC wall specimen with flexure-dominated behavior, and moderately-slender RC wall specimen with significantly pronounced shear-flexure interaction. Comparisons between experimentally measured and analytically predicted load-deformation responses using the model indicated that the *SFI-MVLEM* implemented in OpenSees is capable of capturing reasonably well the hysteretic load-deformation behavior of the RC column and wall specimens considered, by adequately capturing interaction between axial-flexural and shear behavior. Comparisons of the lateral load versus top displacement responses revealed that the proposed modeling approach captures the lateral load capacity, stiffness degradation, and pinching characteristics of RC walls and columns for a range of specimen characteristics (e.g., span-to-depth ratio, axial load level and reinforcing ratio); overestimation of unloading stiffness was observed for only one of the four column specimens considered. A major model shortcoming observed based on the response comparisons is related to the inability of the model to capture strength degradation observed in the experimental results due to model incapability to simulate the experimentally-observed failure mechanisms (e.g., buckling/fracture of reinforcing bars; shear failure).

Future studies could focus on extensive calibration of the analytical model using a large number of test results available in the literature on a broader range of wall and column specimens with different geometries, reinforcement characteristics, and axial load levels, as well as model validation against dynamic tests on building and bridge components and systems. In addition, future research will focus on development and implementation of more robust constitutive models to represent shear transfer mechanisms along the cracks, as well as development and implementation of rebar buckling and fracture behavior into the constitutive relationship for reinforcing steel and constitutive modeling of the sliding shear mechanism above the base of a wall, which would enable the analytical model to capture failure modes associated with these mechanisms. Future work will also include dissemination of research through various training and education activities such as workshops, seminars, and webinars in collaboration with Pacific Earthquake Engineering Research Center (PEER), Earthquake Engineering Research Institute (EERI), and SAVI: Virtual International Institute for Seismic Performance Assessment of Structural Wall Systems.

5. Acknowledgements

This work was supported by the State of California's Transportation Division - Earthquake Risk Reduction Fund through the Pacific Earthquake Engineering Research Center (PEER) Transportation Systems Research Program. Any opinions, findings, and conclusions expressed herein are those of the authors and do not necessarily reflect those of the sponsors. The authors also wish to thank Leonardo Massone, associate professor at the University of Chile, Santiago, and Thien A. Tran, post-doctoral researcher at the University of California, Los Angeles, for his valuable help during the course of this project.

6. References

[1] Massone LM and Wallace JW (2004): Load–deformation responses of slender reinforced concrete walls, American Concrete Institute, *ACI Struct. J*, **101** (1): 103–113.

[2] Thomsen JH and Wallace JW (1995): Displacement-based design of reinforced concrete structural walls: an experimental investigation of walls with rectangular and t-shaped cross-sections, *Report No. CU/CEE-95/06*, Department of Civil Engineering, Clarkson University, Postdam, NY.

[3] Sayre B (2003): Performance Evaluation of Steel Reinforced Shear Walls, *MS Thesis*, Department of Civil and Environmental Engineering University of California, Los Angeles, CA.

[4] Tran TA and Wallace JW (2015): Cyclic Testing of Moderate-Aspect-Ratio Reinforced Concrete Structural Walls," *ACI Struct. J.*, **112** (6)653-665.

[5] Saatcioglu M, Ozcebe G (1989): Response of reinforced concrete columns to simulated seismic loading, American Concrete Institute, *ACI Struct. J.*, **86** (1), 3–12.

[6] Priestley MJN, Seible F, Calvi GM (1996): Seismic Design and Retrofit of Bridges, *John Wiley*, New York, NY.

[7] Massone LM, Orakcal K, Wallace JW (2006): Modeling flexural/shear interaction in RC walls, ACI-SP-236, deformation capacity and shear strength of reinforced concrete members under cyclic loadings, American Concrete Institute, Paper 7: 127–150.

[8] Jiang H, Kurama Y (2010): Analytical modeling of medium-rise reinforced concrete shear walls, American Concrete Institute, *ACI Struct. J.*, **107** (4): 400–410.

[9] Beyer K, Dazio A, Priestley MJN (2011): Shear deformations of slender reinforced concrete walls under seismic loading, American Concrete Institute, *ACI Struct. J.*, **108** (2): 167–177.

[10] Panagiotou M, Restrepo JI, Schoettler M, Kim G (2012): Nonlinear cyclic truss model for reinforced concrete walls, American Concrete Institute, *ACI Struct. J.*, **109** (2): 205–214.

[11] Fischinger M, Rejec K, Isakovic T (2012): Modeling inelastic shear response of RC walls, *15th World Conference on Earthquake Engineering*, Lisbon, Portugal.

[12] Xu S-Y, Zhang J (2010): Hysteretic shear-flexure interaction model of reinforced concrete columns for seismic response assessment of bridges, *Earthq. Eng.Struct. Dyn*., **4** (3): 315–337.

[13] Elwood KJ (2002): Shake Table Tests and Analytical Studies on the Gravity Load Collapse of Reinforced Concrete Frames, *PhD Dissertation*, Department of Civil and Environmental Engineering, University of California, Berkeley.

[14] McKenna F, Fenves GL, Scott MH, and Jeremic B (2000): Open System for Earthquake Engineering Simulation (OpenSees), Pacific Earthquake Engineering Research Center, Berkeley, CA.

[15] Kolozvari K, Orakcal K, Wallace JW (2015a): Modeling of cyclic shear-flexure interaction in reinforced concrete structural walls. i: theory. ASCE, *J. Struct. Eng*., **141** (5): 04014135.

[16] Kolozvari K, Tran T, Orakcal K, Wallace JW (2015b): Modeling of cyclic shear-flexure interaction in reinforced concrete structural walls. ii: experimental validation, ASCE, *J. Struct. Eng*., **141** (5): 04014136.

[17] Kolozvari K, Orakcal K, Wallace JW (2015c): Shear-flexure interaction modeling for reinforced concrete structural walls and columns under cyclic loading, *Technical Report PEER 2015/12*, Pacific Earthquake Engineering Research Institute, Berkeley, USA.

[18] Vulcano A, Bertero VV, Colotti V (1988): Analytical modeling of rc structural Walls, *9th World Conference on Earthquake Engineering*, Tokyo-Kyoto, Japan, (6): 41–46.

[19] Orakcal K, Conte JP, Wallace JW (2004): Flexural modeling of reinforced concrete structural walls - model attributes, American Concrete Institute, *ACI Struct. J.*, **101** (5): 688–698.

[20] Ulugtekin D (2010): Analytical Modeling of Reinforced Concrete Panel Elements under Reversed Cyclic Loadings, *MS Thesis*, Bogazici University, Istanbul, Turkey.

[21] Orakcal K, Massone LM, Ulugtekin D (2012): Constitutive modeling of reinforced concrete panel behavior under cyclic loading, *15th World Conference on Earthquake Engineering*, Lisbon, Portugal.

[22] Chang GA, Mander JB (1994): Seismic energy based fatigue damage analysis of bridge columns: Part I – Evaluation of seismic capacity, *NCEER Technical Report No. NCEER-94-0006*, State University of New York, Buffalo, NY.

[23] Menegotto M, Pinto E (1973): Method of analysis for cyclically loaded reinforced concrete plane frames including changes in geometry and non-elastic behavior of elements under combined normal force and bending, *IABSE Symposium*, Lisbon, Portugal.

[24] Kolozvari K (2013): Analytical Modeling of Cyclic Shear-Flexure Interaction in Reinforced Concrete Structural Walls, *PhD Dissertation*, Department of Civil and Environmental Engineering, University of California, Los Angeles, CA.

[25] Filippou FC, Popov EP, Bertero VV (1983): Effects of bond deterioration on hysteretic behavior of reinforced concrete joints, *Report EERC 83-19*, Earthquake Engineering Research Center, University of California, Berkeley, CA.

[26] Lynn A.C, Moehle J.P. Mahin S.A, Holmes TW (1996): Seismic evaluation of existing reinforced concrete building columns, *Earthquake Spectra*, **12** (4): 715–739.

[27] Orakcal K, Wallace JW (2006): Flexural modeling of reinforced concrete walls - Experimental verification, American Concrete Institute, *ACI Struct. J*, **103** (2): 196–206.

[28] Orakcal K (2004): Nonlinear Modeling and Analysis of Slender Reinforced Concrete Walls, *PhD Dissertation*, Department of Civil and Environmental Engineering, University of California, Los Angeles, CA.